

Solid–Liquid Interfacial Free Energy of Water: A Molecular Dynamics Simulation Study

Jun Wang, Yuk Wai Tang, and X. C. Zeng*

Department of Chemistry, University of Nebraska—Lincoln, Lincoln, Nebraska 68588

Received November 27, 2006

Abstract: The superheating-undercooling hysteresis method and molecular dynamics simulation [Luo et al. *Phys. Rev. B* 2003, 68, 134206] were applied to estimate solid–liquid interfacial free energy (γ) of model water at ambient pressure. Two models of water were selected, the TIP4P-Ew and TIP5P-Ew, which are the improved TIP4P and TIP5P model (for the use with Ewald technique), respectively. The calculated γ at 1 bar is 37 mJ/m² for TIP4P-Ew and 42 mJ/m² for TIP5P-Ew, consistent with a previous direct MD simulation (39 mJ/m²), as well as within the range of measured values (25–44 mJ/m²).

Introduction

The free energy of the interface (γ) at a given pressure is one of the fundamental thermodynamic properties of interfacial systems. For example, the liquid–vapor interfacial free energy (or the surface tension) is relevant to capillary rise, and the solid–liquid interfacial free energy plays an important role in understanding the mechanism of nucleation and crystal growth. Despite its key role in interfacial systems, γ is difficult to measure experimentally. In most cases γ can be measured either indirectly from measurements of crystal nucleation rates or directly by contact angle measurements.¹ The former method is limited by the fact that nucleation primarily occurs heterogeneously, while the latter method has been used to study only a few materials to date due to the difficulty of such experiments.

Theoretically, density-functional theory has been a primary choice to evaluate γ . However, previous studies have been primarily focused on simple model systems (hard-sphere and Lennard-Jones models), and calculations of solid–liquid interfacial free energies are not fully consistent in the literature.^{2–4} Accurate γ can also be obtained through atomistic simulations such as using molecular dynamics (MD). To calculate liquid–vapor surface tension, four types of MD simulation techniques can be selected, including the Kirkwood-Buff mechanical relation, thermodynamic free energy difference, finite-size scaling, and thermodynamic free-energy perturbation.⁵ In the case of solid–liquid interface, however, the mechanical relation method only gives

the excess surface stress, rather than the interfacial free energy γ . Two simulation methods have been developed to compute solid–liquid interfacial free energy γ , namely the fluctuation method and the cleaving potential method. The fluctuation method^{6–9} examines the fluctuations in the height of the interface followed by a Fourier transform to compute the interfacial stiffness which can be fitted to obtain γ . The fluctuation method is able to distinguish weak anisotropy of a system since the anisotropy of the stiffness is an order of magnitude larger than that of the free energy but is less accurate in determining γ due to the fitting process involved. The method cannot be used to resolve faceted interfaces because the fluctuation of interface height is too small. Broughton and Gilmer¹⁰ proposed the cleaving potential method which consists of four reversible steps: cleaving solid phase, cleaving liquid phase, merging solid and liquid interfaces, and removing the fictitious cleaving potential. The total work computed through thermodynamic integration in the four steps is directly related to γ . Davidchack and Laird^{11,12} later proposed to use cleaving walls instead of cleaving potential, which resulted in accuracy sufficient to resolve the anisotropy of interfacial free energy. More recently, Mu and Song¹³ further improved the efficiency of the cleaving potential technique with a multistep thermodynamic perturbation method.

Although both the fluctuation and cleaving potential methods can yield accurate values of solid–liquid interfacial free energy, the simulations are computationally expensive even for simple fluid systems such as hard sphere and Lennard-Jones. An efficient simulation approach to obtain

* Corresponding author e-mail: xczeng@phase2.unl.edu.

Table 1. Comparison of Temperature Hysteresis at Pressure $P = 36.32 \text{ } \epsilon/\sigma^3$ ^a

	T_+ (ϵ/k_B)	T_- (ϵ/k_B)	T_m (ϵ/k_B)	θ_c^+	θ_c^-	β	V_s (σ^3)	V_l	$\Delta H_{m,v}$ (ϵ/σ^3)	γ_{sl} (ϵ/σ^3)	Q (K/ps)
Luo et al. ¹⁵	3.314	1.852	2.688	1.233	0.689	1.954	0.833	0.881	3.380	1.530	8.33
this work	3.14(8)	1.85(6)	2.75(7)	1.24(6)	0.67(4)	2.0(9)	0.828(3)	0.877(4)	3.54(7)	1.6(3)	8.33

^a Extensive quantities are presented per atom. Numbers in parentheses indicate the estimated error on the last digit(s) shown.

orientation averaged value of solid–liquid interfacial free energy is the superheating–undercooling hysteresis method developed by Luo et al.¹⁴ These authors demonstrated that this simulation method can give fair estimation of the solid–liquid interfacial free energy for the Lennard-Jones (LJ) system.¹⁵ They also estimated the interfacial free energy of liquid water/ice system based on experimental undercooling data.¹⁶ Moreover, a direct comparison of solid–liquid interfacial free energy for the LJ system computed from the hysteresis method and the fluctuation method or the cleaving potential technique was also made.¹⁶ The excellent agreement demonstrated the accuracy of the hysteresis method. Here, we employed such a superheating–undercooling hysteresis method to estimate the orientation averaged solid–liquid interfacial free energy of liquid water/ice system, for which the required superheating–undercooling data were obtained from MD simulations with two models of water.

Computational Method

Details of the superheating–undercooling hysteresis method are described elsewhere.¹⁴ The method results in a formula which relates interfacial free energy γ_{sl} with melting temperature T_m , enthalpy change of melting per unit volume $\Delta H_{m,v}$, and a dimensionless nucleation barrier parameter β

$$\gamma_{sl} = \left(\frac{3}{16\pi} \beta k_B T_m \Delta H_{m,v}^2 \right)^{1/3} \quad (1)$$

where k_B is the Boltzmann constant. Based on the classical nucleation theory and undercooling experiments, the maximum superheating $\theta_c^+ = T_+/T_m$ and undercooling $\theta_c^- = T_-/T_m$ can be established as

$$\beta = (A_0 - b \log_{10} Q) \theta_c (1 - \theta_c)^2 \quad (2)$$

where A_0 and b were fitted to be 59.4 and 2.33, respectively, for a number of elements and compounds. The heating/cooling rate Q is normalized by 1 K/s.

We adopted a procedure similar to that reported in the original paper¹⁴ to determine the highest temperature T_+ achievable in a superheated solid and the lowest temperature T_- achievable in an undercooled liquid, before a phase transformation occurs. First, a proton-disordered hexagonal ice I_h is equilibrated at an initial temperature (153.6 K for TIP4P-Ew¹⁷ and 150.5 K for TIP5P-Ew¹⁸) in the MD simulation with the isobaric–isothermal (NPT) ensemble. The temperature and pressure (1 bar) were controlled by using Nose-Hoover¹⁹ technique. Standard periodic boundary conditions were applied in all directions of the orthorhombic box containing 768 water molecules. Both TIP4P-Ew and TIP5P-Ew water molecules were treated as rigid bodies in the MD simulations, and the corresponding rotation equations were solved by using the quaternion algorithm with a time step of 1.0 and 0.5 fs, respectively. Next, the solid (ice) phase

is subjected to incremental heating until it melts. Thereafter, the melt (liquid water) is subjected to incremental cooling. Thermodynamic properties were calculated in every 50 ps heating/cooling step, after a 50 ps run for system equilibration. At the end of each heating/cooling step the temperature was increased or decreased by 3.8 K, corresponding to a heating/cooling rate of 0.076 K/ps. All MD simulations were performed using the DL_POLY2 package.²⁰ The long-range charge–charge interactions were treated with the smooth-particle-mesh-Ewald (SPME) technique.

Results and Discussions

A. Benchmark Test: Melting and Freezing of the Lennard-Jones (LJ) System. We first carried out a benchmark simulation to calculate the solid–liquid interfacial free energy of the LJ system. This test allowed us to examine the feasibility of this approach and to compare results of the unshifted LJ potential obtained in this work with results of the modified LJ potential reported.¹⁵ Only one case ($P=36.32 \text{ } \epsilon/\sigma^3$, where ϵ and σ are the energy and length parameters of LJ potential) was considered for the purpose of comparison. All the simulation parameters were set the same as those reported,¹⁵ except that we used the unshifted LJ potential with a cutoff at 2.5σ . In general, our results are in good agreement with the previous ones,¹⁵ except that we obtained slightly higher values of T_+ and $\Delta H_{m,v}$. A more detailed comparison is shown in Table 1.

B. Solid–Liquid Interfacial Free Energy of TIP4P-Ew and TIP5P-Ew Water. Although homogeneous nucleation has been demonstrated in undercooling experiments, accurate superheating data for ice are rarely reported largely because heterogeneous melting renders measuring the correct superheating limit T_+ difficult. Conversely, homogeneous crystallization of liquid water is rarely reported in MD simulations except for one work.²¹ This is because ice nucleus formation is a rare event in the MD simulation of undercooled water. Similarly, Zheng et al.²² reported that recrystallization of complex molecules by cooling the liquid is very difficult to achieve in MD simulations. Although it is challenging to determine the limiting value of T_- from MD simulation, β and γ_{sl} can be deduced from either T_+ or T_- for given T_m and $\Delta H_{m,v}$. Note that without T_- the melting point T_m cannot be estimated using the formula given in the hysteresis method.¹⁴

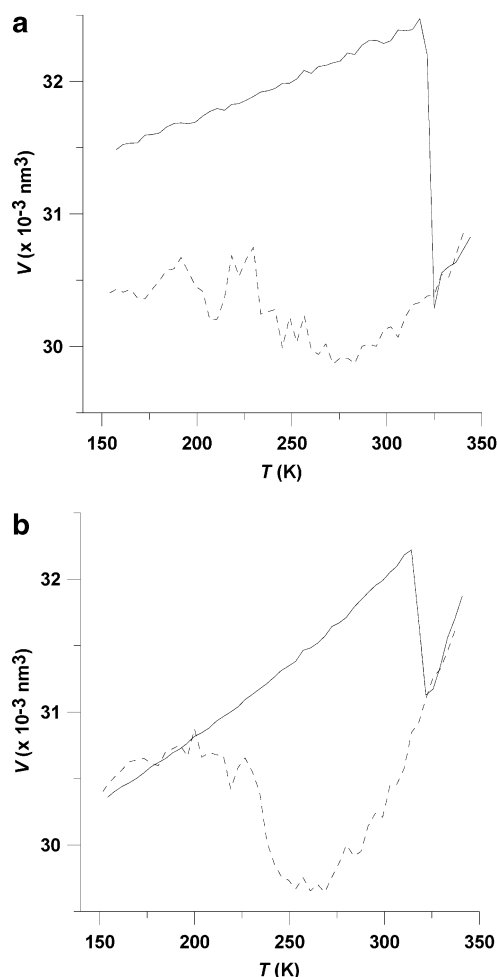
$$T_m = T_+ - \sqrt{T_+ T_-} + T_- \quad (3)$$

However, the equilibrium melting temperature T_m for both TIP4P-Ew and TIP5P-Ew water models can be determined using other independent computational approach, for example, the two-phase coexistence approach reported previously.^{23–24} ΔH_m can be calculated from the enthalpy difference between the solid and liquid at T_m , while $\Delta H_{m,v}$

Table 2. Comparison of Calculated Interfacial Free Energy at $P = 1$ Bar for the Two Water Models^a

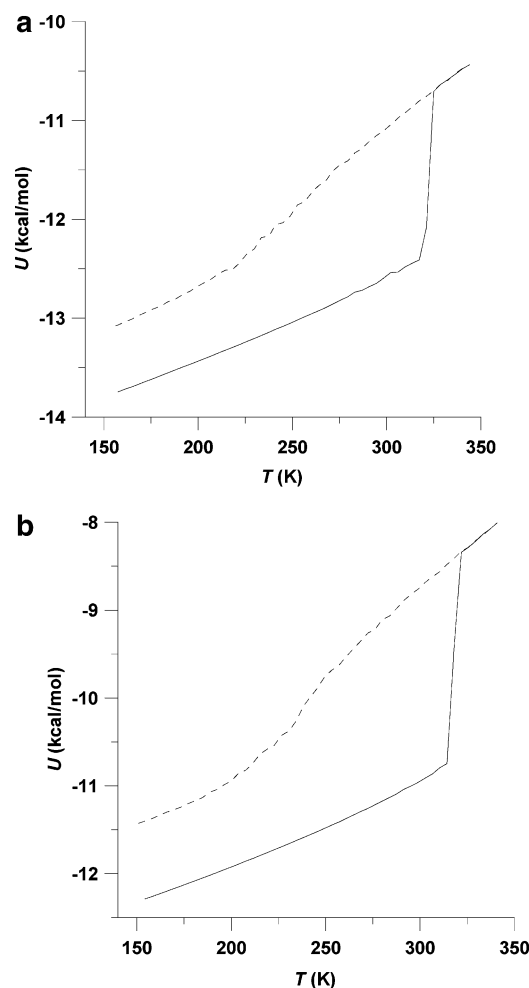
	T_+ (K)	T_m (K)	θ_c^+	β	V_s (Å ³)	V_l (Å ³)	$\Delta H_{m,v}$ ($\times 10^8$ J/m ³)	γ_{sl} (mJ/m ²)	Q (K/ps)
TIP4P-Ew	321(6)	244(1) ^b	1.32(3)	4.5(9)	32.0(1)	30.2(2)	2.40(5)	37(3)	0.0762
TIP4P-Ew	317(7)	244(1) ^b	1.30(4)	4.1(9)	32.0(1)	30.2(2)	2.40(5)	36(3)	0.0200
TIP5P-Ew	314(6)	254(1)	1.24(3)	2.4(7)	31.4(1)	29.9(3)	3.90(7)	42(4)	0.0762
TIP5P-Ew	314(6)	254(1)	1.24(3)	2.5(7)	31.4(1)	29.9(3)	3.90(7)	42(4)	0.0200

^a Extensive quantities are presented per molecule. Numbers in parentheses indicate the estimated error on the last digit(s) shown. ^b The melting temperature of TIP4P-Ew ice is updated from the previously reported value 257.0 K²³ to 244 ± 1 K based on a much longer (1 ns) two-phase-coexistence (in NPT ensemble) simulation with 12 288 water molecules. This new T_m value is very close to the result of $T_m = 242$ K reported by Fernandez et al.²⁴ using the same simulation method and a smaller system. The previously reported melting point 254 ± 1 K of TIP5P-Ew ice remains the same on basis of the longer (1 ns) simulation in NPT ensemble (see Supporting Information, Figure S3), about 16 K lower than $T_m = 270$ K reported by Fernandez et al.²⁴ Assuming $T_m = 270$ K, we also estimated the corresponding interfacial free energy for TIP5P-Ew, which is 36 mJ/m² (see Supporting Information, Table S1).

**Figure 1.** Temperature dependence of volume ($Q=0.0762$ K/ps) for (a) the TIP4P-Ew model and (b) the TIP5P-Ew model. Solid line represents superheating, and dashed line represents undercooling.

is normalized to the average volume of solid and liquid at the melting temperature.

As expected, upon superheating, the volume of solid ice gradually increases with increasing the temperature before a sudden reduction of the volume (due to the collapse of ice structure) (Figure 1). This behavior is unique in heating tetrahedral structure materials.²⁵ Near the superheating limit, there is an obvious potential energy jump (Figure 2) as well as one order-of-magnitude increase of diffusion coefficient (Figure 3). These observations confirmed that melting occurs at 321 K for TIP4P-Ew and 314 K for TIP5P-Ew. Moreover,

**Figure 2.** (a) Temperature dependence of potential energy ($Q=0.0762$ K/ps) for (a) the TIP4P-Ew model and (b) the TIP5P-Ew model. Solid line represents superheating and dashed line represents undercooling.

additional simulations using the constant stress-constant temperature ensemble and NPT ensemble with 2592 water molecules were performed to ensure that the superheating limit is not very sensitive to system size and box shape (Supporting Information, Figures S1 and S2). Although the diffusion coefficient of liquid water can decrease to the same magnitude as that of I_h ice below 210 K upon undercooling (Figure 3), no ordered structure was observed from the analysis of configuration snapshots at the low temperatures. A stiffer undercooling curve of volume change is obtained for TIP5P-Ew (Figure 1) but still not sufficient to locate T_-

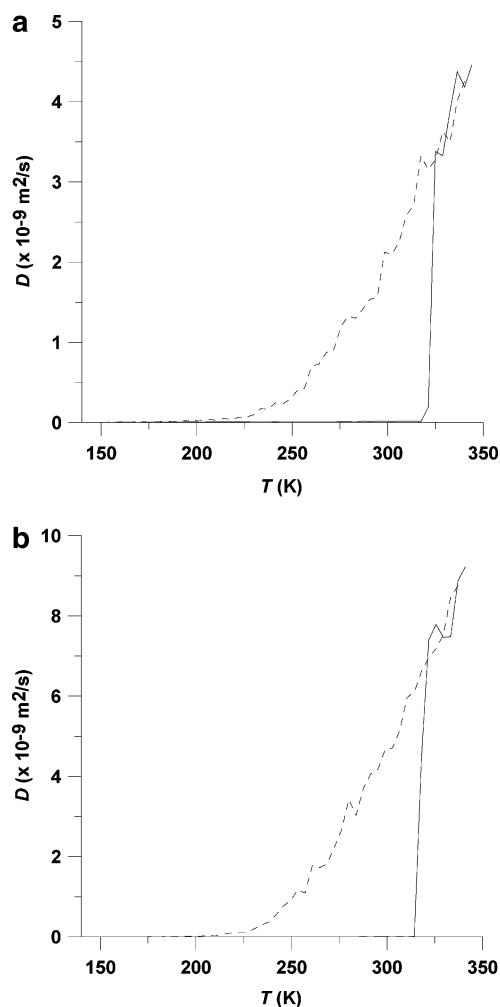


Figure 3. Temperature dependence of diffusion coefficient ($Q=0.0762\text{K/ps}$) for (a) the TIP4P-Ew model and (b) the TIP5P-Ew model. Solid line represents superheating and dashed line represents undercooling.

due to the continuous decrease of potential energy (Figure 2). The volume of liquid water eventually fluctuates near a constant after a slow increase from 280 to 230 K (Figure 1). Based on the temperature dependence of radial distribution function (Figure 4) the liquid water may undergo a continuous transformation toward an amorphous ice upon undercooling.

The calculated interfacial free energies γ_{sl} with two different heat/cooling rates for two water models are shown in Table 2. It appears that the heating/cooling rate has little effect on the calculated γ_{sl} . Overall, the calculated γ_{sl} are consistent with a previous MD simulation result²⁶ (39 mJ/m^2) as well as within the range of measured values¹⁶ ($25\sim 44\text{ mJ/m}^2$). Conversely, both TIP4P-Ew and TIP5P-Ew models give rise to higher γ_{sl} compared to the result (28.0 mJ/m^2)¹⁶ and direct measurement of solid–liquid interfacial energy²⁷ (29.1 mJ/m^2). The discrepancy may be due in part to the empirical TIP4P-Ew and TIP5P-Ew models of water employed in this work. For example, both models underestimate the melting temperatures of water, which renders the material dependent parameter β larger by a factor of 4 (two for TIP5P-Ew) compared to the reported value¹⁶ (1.0).

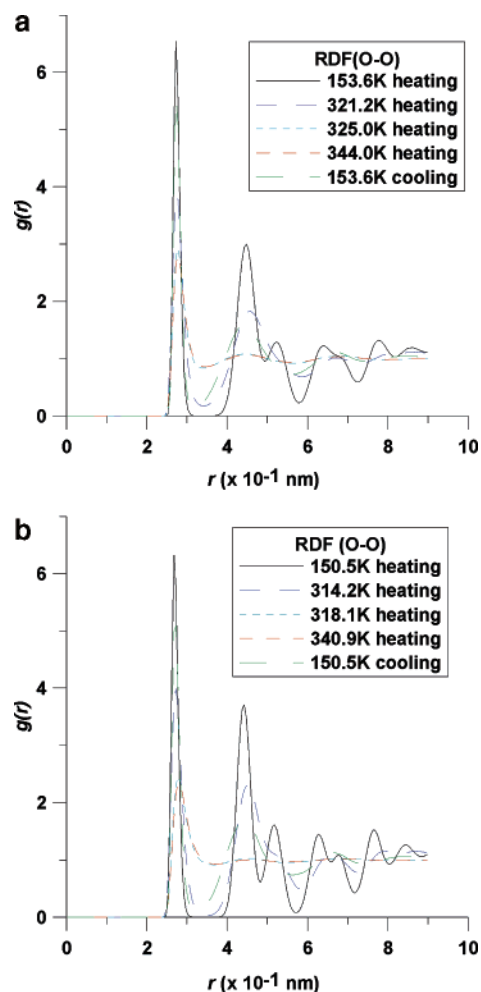


Figure 4. Temperature dependence of radial distribution function of oxygen atoms ($Q=0.0762\text{K/ps}$) for (a) the TIP4P-Ew model and (b) the TIP5P-Ew model.

Conclusion

In summary, we employed the Luo et al.'s method¹⁴ and superheating/undercooling data directly from MD simulations to estimate the solid–liquid interfacial free energy γ_{sl} of liquid water/ice interface with two water models. With the melting temperature T_{m} obtained from independent simulations,^{23,24} the calculated γ_{sl} are consistent with a previous direct MD simulation²⁵ but appreciably higher than the results obtained based on experimental undercooling data.¹⁶ More accurate values of the liquid water/ice interfacial free energy for the two model systems can be computed by using either the fluctuation or cleaving potential method. Research in this direction is under way.

Acknowledgment. We are grateful to Professor J. R. Morris and Professor X. Y. Song for valuable discussions. This research was supported by grants from DOE (DE-FG02-04ER46164), NSF (CHE-0427746 and CHE-0701540), John Simon Guggenheim Foundation, the Nebraska Research Initiative (X.C.Z.), and by the Research Computing Facility at University of Nebraska–Lincoln.

Supporting Information Available: Figures S1–S3 and Table S1. This material is available free of charge via the Internet at <http://pubs.acs.org>.

References

- (1) Woodruff, D. P. The experimental determination of the solid-liquid interfacial free energy. In *The Solid-Liquid Interface*, 1st ed.; Cahn, R. W., Forty, A. J., Ward, I. M., Eds.; Cambridge University Press: London, U.K., 1973; Vol. 2, pp 12–31.
- (2) McMullen, W. E.; Oxtoby, D. W. *J. Chem. Phys.* **1988**, *88*, 1967.
- (3) Curtin, W. A. *Phys. Rev. Lett.* **1987**, *59*, 1228.
- (4) Marr, D. W.; Gast, A. P. *Phys. Rev. E* **1993**, *47*, 1212.
- (5) Gloor, G. J.; Jackson, G.; Blas, F. J.; de Miguel, E. *J. Chem. Phys.* **2005**, *123*, 134703.
- (6) Hoyt, J. J.; Asta, M.; Karma, A. *Phys. Rev. Lett.* **2001**, *86*, 5530.
- (7) Morris, J. R. *Phys. Rev. B* **2002**, *66*, 144104.
- (8) Asta, M.; Hoyt, J. J.; Karma, A. *Phys. Rev. B* **2002**, *66*, 100101.
- (9) Morris, J. R.; Song, X. *J. Chem. Phys.* **2003**, *119*, 3920.
- (10) Broughton, J. Q.; Gilmer, G. H. *J. Chem. Phys.* **1986**, *84*, 5759.
- (11) Davidchack, R. L.; Laird, B. B. *Phys. Rev. Lett.* **2000**, *85*, 4751.
- (12) Davidchack, R. L.; Laird, B. B. *J. Chem. Phys.* **2003**, *118*, 7651.
- (13) Mu, Y.; Song, X. *J. Chem. Phys.* **2006**, *124*, 034712.
- (14) Luo, S. N.; Ahrens, T. J.; Cagin, T.; Strachan, A.; Goddard, W. A., III; Swift, D. C. *Phys. Rev. B* **2003**, *68*, 134206.
- (15) Luo, S. N.; Strachan, A.; Swift, D. C. *J. Chem. Phys.* **2004**, *120*, 11640.
- (16) Luo, S. L.; Strachan, A.; Swift, D. C. *Modell. Simulat. Mater. Sci. Eng.* **2005**, *13*, 321.
- (17) Horn, W.; Swope, W. C.; Pitera, J. W.; Madura, J. C.; Dick, T. J.; Hura, G. L.; Head-Gordon, T. *J. Chem. Phys.* **2004**, *120*, 9665.
- (18) Rick, S. W. *J. Chem. Phys.* **2004**, *120*, 6085.
- (19) Melchionna, S.; Ciccotti, G.; Holian, B. L. *Mol. Phys.* **1993**, *78*, 533.
- (20) Smith, W.; Forester, T. R. *DL_POLY_2.15*; Daresbury Laboratory: Cheshire, U.K. 2003.
- (21) Matsumoto, M.; Saito, S.; Ohmine, I. *Nature* **2002**, *416*, 409.
- (22) Zheng, L. Q.; Luo, S. N.; Thompson, D. L. *J. Chem. Phys.* **2006**, *124*, 154504.
- (23) Wang, J.; Yoo, S.; Bai, J.; Morris, J. R.; Zeng, X. C. *J. Chem. Phys.* **2005**, *123*, 036101.
- (24) Fernandez, R. G.; Abascal, J. L. F.; Vega, C. *J. Chem. Phys.* **2006**, *124*, 144506.
- (25) Tang, Y. W.; Wang, J.; Zeng, X. C. *J. Chem. Phys.* **2006**, *124*, 236103.
- (26) Haymet, A. D. J.; Bryk, T.; Smith, E. J. Solute Ions at Ice/Water Interface. In *Ionic Soft Matter: Modern Trends in Theory and Applications*; Proceedings of the NATO Advanced Research Workshop on Ionic Soft Matter, Lviv, Ukraine, April 14–17, 2004; Henderson, D., Holovko, M., Trokhymchuk, A., Eds.; Springer: London, 2005; pp 333–359.
- (27) Hardy, S. C. *Philos. Mag.* **1977**, *35*, 471.

CT600345S